

Luminescent Zinc(II) Complexes of Fluorinated Benzothiazol-2-yl Substituted Phenoxide and Enolate Ligands

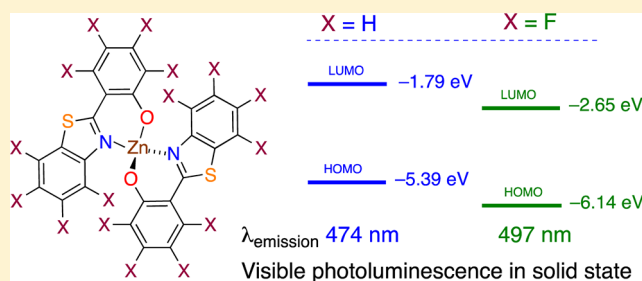
Zhe Li,^{†,‡} Ahmed Dellali,[†] Jahangir Malik,[†] Majid Motevalli,[†] Roger M. Nix,[†] Toyin Olukoya,[†] Yu Peng,^{†,‡} Huangqing Ye,[‡] William P. Gillin,[‡] Ignacio Hernández,[‡] and Peter B. Wyatt^{*,†}

[†]Materials Research Institute, School of Biological and Chemical Sciences, Queen Mary University of London, Mile End Road, London, United Kingdom E1 4NS

[‡]Materials Research Institute, School of Physics and Astronomy, Queen Mary University of London, Mile End Road, London, United Kingdom E1 4NS

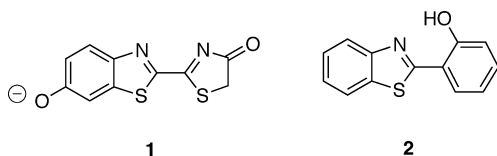
S Supporting Information

ABSTRACT: Zn(II) complexes of the following new, fluorine-containing, benzothiazole-derived ligands have been synthesized and characterized crystallographically: 2-(3,3,3-trifluoro-2-oxopropyl)benzothiazole (3), 4,5,6,7-tetrafluoro-2-(3,3,3-trifluoro-2-oxopropyl)benzothiazole (4), 4,5,6,7-tetrafluoro-2-(2-hydroxyphenyl)benzothiazole (12), 2-(3,4,5,6-tetrafluoro-2-hydroxyphenyl)-4,5,6,7-tetrafluorobenzothiazole (13), and 2-(3,4,5,6-tetrafluoro-2-hydroxyphenyl)benzothiazole (16); the Cu(II) complex of ligand 4 is also reported. These are analogs of the important photo- and electroluminescent material [Zn(BTZ)₂]₂, where H-BTZ = 2-(2-hydroxyphenyl)benzothiazole. DFT calculations indicate that HOMO and LUMO energy levels in these materials are substantially lowered by fluorination. The fluorinated ZnL₂ complexes are mononuclear (in contrast to the dinuclear, nonfluorinated material [Zn(BTZ)₂]₂). They easily sublime and show broad visible photoluminescence. A common crystallographic feature is the existence of pairs of fluorinated ZnL₂ molecules related by inversion centers, with their π systems facing one another.



INTRODUCTION

The luminescence of benzothiazole derivatives is exploited both by nature and by human technology. Thus, the phenolate of oxyluciferin (1) is responsible for light emission in fireflies and other bioluminescent insects,¹ whereas the zinc(II) complex of 2-(2-hydroxyphenyl)benzothiazole (H-BTZ, 2) is an excellent white-light emitting material for organic light-emitting diodes (OLEDs).^{2–4} The dimeric [Zn(BTZ)₂]₂ structure has five-coordinate zinc centers connected by bridging oxygen atoms from the BTZ ligands. Recently, the effects of introducing additional alkyl, alkoxy, and aryl substituents into the structure of ligand 2 have been examined both experimentally and computationally, resulting in changes to the energies of molecular orbitals in the zinc complexes and shifts in the wavelengths of their maximum light emission.^{5,6}



Fluorine atoms possess high electronegativity, small size, and the ability to form strong bonds to carbon. Consequently, fluorinated aromatic compounds combine a readiness to accept electrons with good chemical stability, making materials such as

perfluoropentacene⁷ of interest in organic electronics. In addition, fluorination is expected to modify both optical and structural properties of organic materials: the replacement of hydrogen by fluorine leads to significantly enhanced spin–orbit coupling,⁸ while perfluorinated ligands lack high energy C–H vibrational modes that can cause nonradiative quenching of IR luminescence, e.g., from Er³⁺ ions.⁹ The π – π_F interaction between fluorinated and nonfluorinated aromatic rings is recognized as being mediated by a combination of dispersion and Coulombic noncovalent forces,¹⁰ strongly favoring the parallel alignment of aryl and perfluoroaryl groups and so directing the self-assembly of materials that contain both types of ring.

We now describe the synthesis of both partially and fully fluorinated metal-containing organic materials, incorporating benzothiazole-derived ligands, and examine the effects of fluorination on the structures and properties of these complexes.

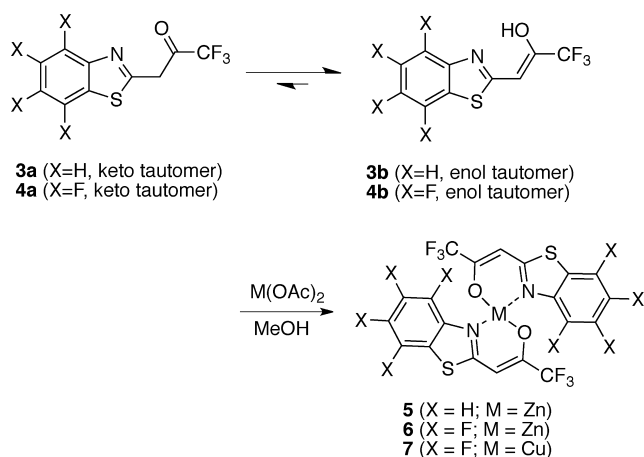
RESULTS AND DISCUSSION

Synthesis and Characterization. 2-(3,3,3-Trifluoro-2-oxopropyl)benzothiazole (3) is easily prepared by the reaction of commercially available 2-methylbenzothiazole with trifluoro-

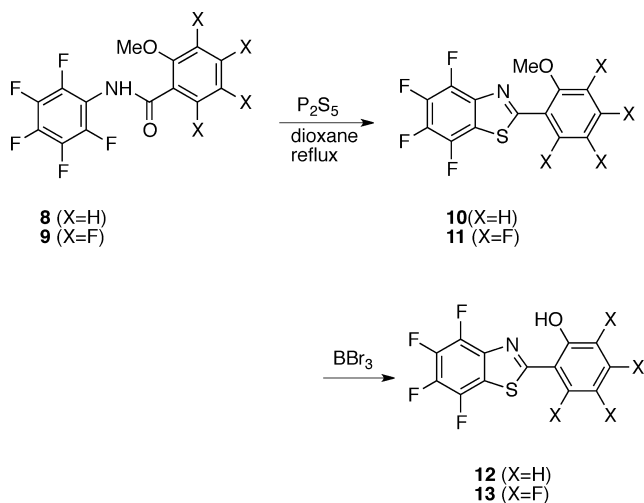
Received: September 23, 2012

Published: January 14, 2013

acetic anhydride and pyridine.¹¹ 4,5,6,7-Tetrafluoro-2-methylbenzothiazole, itself obtained by cyclizing 2,3,4,5,6-pentafluoroacetanilide using phosphorus(V) sulfide,¹² was trifluoroacetylated using ethyl trifluoroacetate and sodium hydride in THF to give 4,5,6,7-tetrafluoro-2-(3,3,3-trifluoro-2-oxopropyl)-benzothiazole (**4**). ¹H NMR and IR spectra indicate that ligands **3** and **4** exist very largely as their enol tautomers. The reaction of **3** and **4** with methanolic zinc(II) acetate led to the precipitation of the corresponding zinc(II) complexes **5** and **6**. In the case of the new, highly fluorinated ligand **4**, we also prepared the copper(II) complex **7** by similar means.

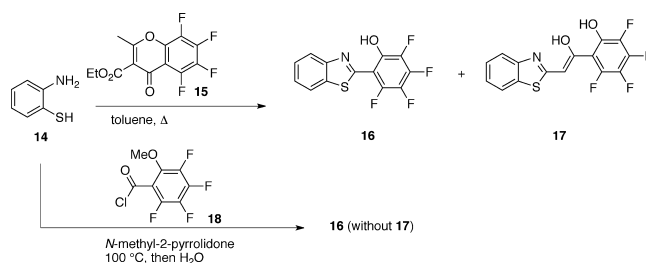


Acylation of pentafluoroaniline using 2-methoxybenzoyl chloride gave the amide **8**, which was converted into 4,5,6,7-tetrafluoro-2-(2-methoxyphenyl)benzothiazole (**10**) by cyclization with phosphorus(V) sulfide, followed by demethylation with BBr₃ to give ligand **12**. The fully fluorinated ligand **13** was prepared similarly to **12**, except that the acylation of pentafluoroaniline was performed using 3,4,5,6-tetrafluoro-2-methoxybenzoyl chloride.

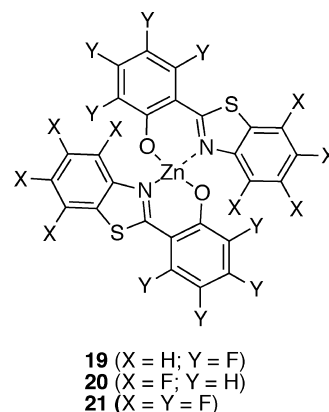


The preparation of 2-(2-hydroxy-3,4,5,6-tetrafluorophenyl)-benzothiazole (**16**) has previously been reported, by reaction of the 2-aminothiophenol **14** with the chromone derivative **15**.¹³ However, the literature ¹H NMR of **16** has two separate OH signals at low field, with the entire aromatic region described as one multiplet. When we attempted to replicate this preparation, we isolated, after purification by flash chromatography, a low yield of material that had a ¹H NMR spectrum consistent with that of structure **16**, with only one OH signal and four distinct

aromatic C–H environments; the melting point was more than 30° higher than the literature value, but ¹⁹F NMR and high resolution mass spectrometry were also consistent with our isolation of **16** as a single entity. It is therefore likely that the material previously described by Bazyl' et al.¹³ was not pure **16**. We identified benzothiazole derivative **17** as an additional product of the reaction between **14** and **15**, isolable by recrystallization of the crude product. In an attempt to increase the yield of **16**, we tried condensing 2-aminothiophenol with 3,4,5,6-tetrafluoro-2-methoxybenzoyl chloride (**18**) in hot *N*-methyl-2-pyrrolidone (NMP), using the general approach of Brembilla et al.¹⁴ We were pleased to find that *O*-demethylation occurred under these reaction conditions, to give the required phenol **16** in a one-pot reaction after quenching with water.



The zinc complexes **19** and **20**, which are fluorinated analogues of Zn(BTZ)₂, precipitated from methanol upon mixing solutions of zinc(II) acetate and potassium salts of the ligands. Complex **21** is comparatively soluble in methanol and so was prepared by precipitation from aqueous solution.



X-Ray Crystallography. Crystals of the enolate complexes **5**, **6**, and **7** for X-ray diffraction were obtained by recrystallization from CHCl₃, EtOAc–Et₂O, and EtOH–Et₂O, respectively; X-ray quality crystals of the phenoxide complexes **19**, **20**, and **21** were grown by vacuum sublimation in a sealed glass tube (with a pressure below 10^{–6} mbar, temperature between 250 and 300 °C). Single crystal X-ray diffraction studies were performed on all six metal complexes (Figures 1 and 2 and Supporting Information). Structures were solved and refined using the Bruker SHELXTL Software Package.

Table 1 summarizes the crystallographic details, while Table 2 presents bond lengths and angles relating to the coordination of the metal centers. In contrast to the dimeric [Zn(BTZ)₂]₂, molecules of which possess an inversion center, all six metal complexes have mononuclear structures, where two ligands chelate the central, four-coordinate metal ion using the benzothiazole nitrogen atom and the oxygen of the enolate or phenoxide group. The effect of fluorination on reducing nuclearity may be attributed to the resulting reduction in the

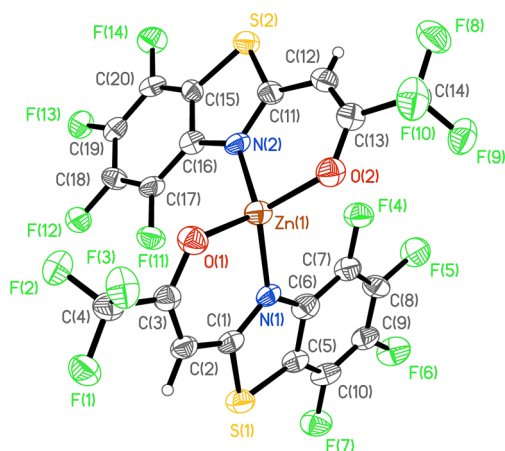


Figure 1. Molecular structure of enolate complex **6**. Ellipsoids are shown at the 50% probability level.

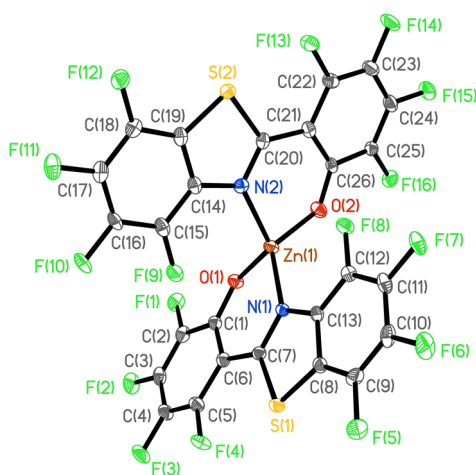


Figure 2. Molecular structure of phenoxide complex **21**.

Lewis basicity of the ligands, as has previously been proposed, e.g., for lanthanide perfluorarylthiolate complexes¹⁵ and for Co(II) and Cu(II) pentafluorophenoxides.¹⁶

All six fluorinated metal complexes exist in the solid state as chiral molecules that crystallize as racemic compounds in centrosymmetric space groups. The enolate and phenoxide units in the coordinated ligands are approximately coplanar with the benzothiazole ring system, with N–C–C–C torsion angles of less than 10°. The four-coordinate zinc complexes **5**, **6**, **19**, **20**, and **21** have roughly tetrahedral geometries, with shorter Zn–O and Zn–N bond lengths and larger O–Zn–N angles than in the five coordinate [Zn(BTZ)₂]₂. The copper(II) complex **7** shows greater distortion from tetrahedral geometry than the analogous zinc complex **6**; in particular the N(1)–Cu–N(2) angle in **7** is larger, and the O–Cu–N angle is smaller, than the corresponding values in **6**.

Mixtures of arenes and perfluoroarenes with a 1:1 molar ratio,¹⁷ as well as single substances such as 1,2,3,4-tetrafluoronaphthalene,¹⁸ often adopt crystal structures containing parallel stacks of Ar(H) and Ar(F) rings. These π – π_F interactions, which are estimated to be stabilizing to the extent of 20–25 kJ mol^{−1}, provide a strong influence for directing molecular assembly but may be outweighed by other effects, including hydrogen bonding and steric repulsion.¹⁰ It is therefore of interest to examine the nature of the π – π

interactions that occur within the series of zinc phenoxide complexes. In considering these stacking interactions, it should be noted that precise values of calculated interplanar separations are influenced by the choice of atoms used to define the molecular plane.¹⁹

For [Zn(BTZ)₂]₂, each dimer molecule contains four nearly planar benzothiazole units, which are used to engage in pairwise π – π interactions with four neighboring molecules, creating a three-dimensional network. These interactions take place in two approximately mutually perpendicular directions, so that terminal ligands pair with other terminal ligands of adjacent dimer molecules (the literature reported² interplanar separation of 3.77 Å is equal to the distance between the mean planes of the six carbon atoms in the carbocyclic “benzo” ring of the benzothiazole), while bridging ligands pair with neighboring bridging ligands (separation 3.60 Å). The zinc phenoxide structures **19**, **20**, and **21** all contain pairs of neighboring zinc complexes that are related by centers of inversion and have π -systems facing one another in an antiparallel alignment. In the case of **19**, these rings are offset so that the nonfluorinated, carbocyclic “benzo” portions of the benzothiazole units are aligned and the substituents on these rings eclipse those on their neighbors (Figure 3). The separation of the planes of these rings is 3.63 Å, and the distance between the centroids of the nonfluorinated rings is 3.64 Å. These parallel aromatic rings are parts of infinite stacks in which two nonfluorinated rings are followed by two fluorinated rings. Thus, π_H – π_H , π_H – π_F , and π_F – π_F interactions all exist within the stacks (Figure 4). The separation between the planes of the nonfluorinated rings and the centroids of neighboring fluorinated rings is 3.36 Å, while that between the planes of adjacent fluorinated rings is 3.28 Å. Structure **19** additionally contains infinite stacks of aromatic rings in which neighboring molecules are related by a *c* glide. These stacks are approximately perpendicular to planes formed by the eclipsed “benzo” rings in **19** that are referred to above. Within the stacks, the fluorinated phenol rings roughly face each other, as do the nonfluorinated benzothiazole units, with a mean interplanar spacing of 3.54 Å. However, neighboring rings are not perfectly parallel, and they approach within 3.5 Å of one another.

In **20**, the nonfluorinated phenoxide rings face the fluorinated benzothiazole units so that the C–H and C–F bonds of the opposing rings are staggered, forming infinite stacks. The interplanar separation alternates so that it is 3.23 Å in pairings where the nonfluorinated phenol lies over both rings of the fluorinated benzothiazole, compared with 3.59 Å when the phenol is positioned to one side of the fluorinated carbocyclic ring of the benzothiazole. Infinite stacks that form in an approximately perpendicular direction (mean interplanar separation 3.44 Å) also juxtapose fluorinated and nonfluorinated aromatic components, although in this case the extent of overlap of the rings is comparatively small.

In the fully fluorinated system **21** (space group *P* $\bar{1}$), phenoxide rings face the fluorinated benzothiazoles across inversion centers with the C–F bonds out of register and a separation between planes of 3.32 Å (based on the mean separation of the centroid of one ring and the plane defined by the carbon atoms of the facing ring). In an approximately perpendicular direction, infinite stacks form with an interplanar separation of 3.20 Å. The stacks are displaced laterally so that the phenol ring of one molecule faces the carbocyclic part of the benzothiazole system in the neighboring molecule with 3.62 Å separation of the ring centroids.

Table 1. Crystallographic Details of Enolate and Phenoxide Complexes

compound	5	6	7	19	20	21
CCDC number ^a	873934	873936	873935	873933	873932	873937
formula	C ₂₀ H ₁₀ F ₆ N ₂ O ₂ S ₂ Zn	C ₂₀ H ₂ F ₁₄ N ₂ O ₂ S ₂ Zn	C ₂₀ H ₂ CuF ₁₄ N ₂ O ₂ S ₂	C ₂₆ H ₈ F ₈ N ₂ O ₂ S ₂ Zn	C ₂₆ H ₈ F ₈ N ₂ O ₂ S ₂ Zn	C ₂₆ F ₁₆ N ₂ O ₂ S ₂ Zn
fw	553.79	697.73	695.90	661.83	661.83	805.77
temp	120(2) K	120(2) K	120(2) K	100(2) K	100(2) K	100(2) K
cryst syst	triclinic	monoclinic	triclinic	monoclinic	monoclinic	triclinic
space group	$P\bar{1}$	$P2_1/n$	$P\bar{1}$	$P2_1/c$	$P2_1/n$	$P\bar{1}$
<i>a</i>	7.7002(2) Å	10.6956(14) Å	8.6220(3) Å	12.6004(4) Å	7.350(5) Å	7.7232(2) Å
<i>b</i>	11.0829(3) Å	11.254(2) Å	11.3026(3) Å	24.1084(8) Å	25.035(5) Å	11.8735(3) Å
<i>c</i>	12.3763(4) Å	19.077(3) Å	12.5469(4) Å	7.5640(3) Å	12.638(5) Å	13.9100(4) Å
α	75.809 (1)°	90°	68.841(2)°	90°	90°	92.4460(10)°
β	79.705(2)°	103.523(9)°	84.985(2)°	97.393(2)°	100.733(5)°	103.5580(10)°
γ	82.847(2)°	90°	77.252(2)°	90°	90°	93.9180(10)°
<i>V</i>	1003.87(5) Å ³	2232.6(6) Å ³	1112.13(6) Å ³	2278.66(14) Å ³	2284.8(19) Å ³	1234.85(6) Å ³
<i>Z</i>	2	4	2	4	4	2
density (calculated)	1.832 Mg/m ³	2.076 Mg/m ³	2.078 Mg/m ³	1.929 Mg/m ³	1.924 Mg/m ³	2.167 Mg/m ³
absorption coeff	1.509 mm ⁻¹	1.430 mm ⁻¹	1.313 mm ⁻¹	4.127 mm ⁻¹	1.356 mm ⁻¹	1.320 mm ⁻¹
cryst size	0.36 × 0.24 × 0.06 mm ³	0.28 × 0.14 × 0.02 mm ³	0.26 × 0.08 × 0.04 mm ³	0.08 × 0.10 × 0.20 mm ³	0.10 × 0.12 × 0.16 mm ³	0.12 × 0.14 × 0.24 mm ³
reflns collected	18261	20098	22507	36422	39802	22725
independent reflns	4593 [R(int) = 0.0499]	4365 [R(int) = 0.1296]	5099 [R(int) = 0.0681]	4003 [R(int) = 0.0439]	3779 [R(int) = 0.0306]	5027 [R(int) = 0.0142]
final R indices [I > 2 σ (I)]	R1 = 0.0356 wR2 = 0.0795	R1 = 0.0780 wR2 = 0.1609	R1 = 0.0474 wR2 = 0.1073	R1 = 0.0284 wR2 = 0.0775	R1 = 0.0398 wR2 = 0.1037	R1 = 0.0428 wR2 = 0.1129
R indices (all data)	R1 = 0.0474 wR2 = 0.0849	R1 = 0.1312 wR2 = 0.1853	R1 = 0.0725 wR2 = 0.1188	R1 = 0.0308 wR2 = 0.0791	R1 = 0.0442 wR2 = 0.1074	R1 = 0.0439 wR2 = 0.1138

^aCrystallographic data (excluding structure factors) have been deposited with the Cambridge Crystallographic Data Centre as supplementary publications with the indicated CCDC numbers. Copies of the data can be obtained free of charge on application to CCDC, 12 Union Road, Cambridge CB2 1EZ; e-mail: deposit@ccdc.cam.ac.uk.

Table 2. Selected Experimental Bond Lengths (Å) and Angles (deg) for Metal Complexes

compound	5	6	7	19	20	21
M(1)–O(1)	1.9283(16)	1.935(5)	1.905(2)	1.9131(15)	1.912(3)	1.907(2)
M(1)–O(2)	1.9525(16)	1.919(5)	1.903(2)	1.9090(14)	1.912(3)	1.893(2)
M(1)–N(1)	2.0005(19)	2.003(6)	1.947(2)	1.9944(17)	2.020(3)	2.020(2)
M(1)–N(2)	1.9913(19)	2.003(6)	1.958(2)	1.9899(17)	2.017(3)	2.036(3)
O(1)–M(1)–N(1)	95.14(7)	95.7(2)	94.78(9)	93.68(7)	94.00(11)	93.01(10)
O(2)–M(1)–N(2)	96.28(7)	96.8(2)	94.78(10)	94.05(7)	93.31(11)	93.39(10)
O(1)–M(1)–O(2)	127.11(7)	112.0(2)	137.19(10)	118.19(7)	123.27(11)	107.57(10)
N(1)–M(1)–N(2)	119.71(7)	116.4(2)	151.77(11)	131.87(7)	134.70(12)	116.29(10)
O(1)–M(1)–N(2)	114.27(8)	117.7(2)	95.36(10)	110.68(6)	105.65(11)	121.46(10)
O(2)–M(1)–N(1)	106.09(7)	119.8(2)	95.51(9)	110.47(6)	109.47(11)	127.53(10)

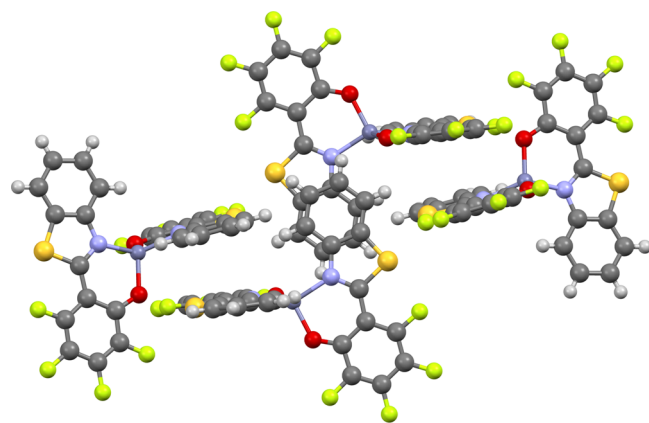


Figure 3. Intermolecular contacts in the crystal structure of **19**, showing π_H – π_H and π_F – π_F stacking.

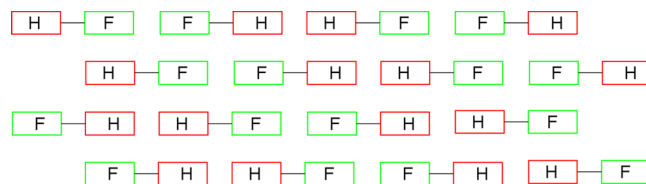


Figure 4. Stacking of ligand π systems within crystals of **19**, indicating the relative positions of fluorinated (green) and nonfluorinated (red) aromatic rings.

Thus, the existence of stacked π systems is a feature of all the phenoxide complexes. Despite the importance of π_H – π_F interactions in simple organic structures where such interactions are possible and its presence in **20**, this particular type of π -stacking is not the only one observed for half-fluorinated systems such as **19**. However, *all* of these systems form centrosymmetric structures derived from chiral monomers.

Thus, the strongest influence in dictating the architecture of these crystals is the mutual recognition of enantiomers brought about by the favorable interaction of oppositely directed electrical dipoles, not the attraction of fluoroaryl groups for their fluorine-free counterparts.

Photophysical Studies on Metal Complexes. *a. Solution Phase Absorption.* The zinc enolate complexes **5** and **6** are colorless, with strong absorption peaks at 342 and 347 nm, respectively, in acetonitrile solution (Figure 5). The copper

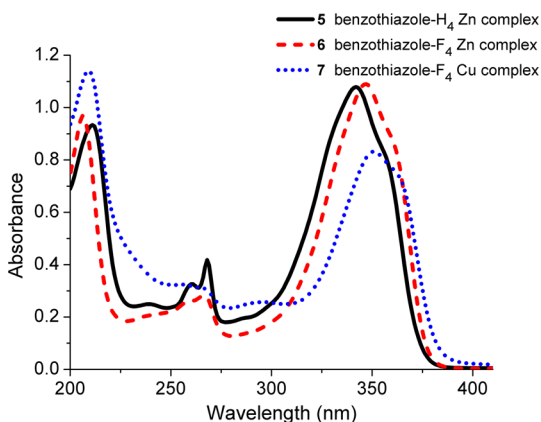


Figure 5. UV spectra of metal enolates **5**, **6**, and **7** (2×10^{-5} M solutions in MeCN).

complex **7** is deep purple to the eye, but its visible absorption peaks have extinction coefficients below 100, while in the UV region its absorption spectrum is similar to those of **5** and **6**. The fluorinated zinc phenoxides **19**, **20**, and **21** are yellow and have solution phase absorption spectra (recorded in DMSO) that are qualitatively similar to one another (Figure 6). All the

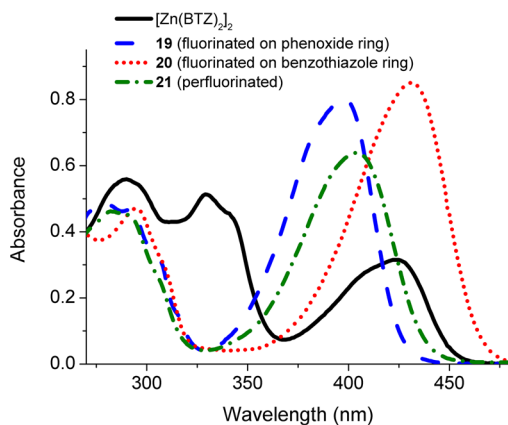


Figure 6. UV-visible spectra of zinc phenoxides $[\text{Zn}(\text{BTZ})_2]_2$, **19**, **20**, and **21** (2×10^{-5} M with respect to Zn^{2+} , solutions in DMSO).

phenoxides, including $[\text{Zn}(\text{BTZ})_2]_2$, have their longest wavelength absorptions in the blue region. The fluorinated phenoxides, which are mononuclear in the solid state, lack an absorption peak corresponding to the UV absorption of $[\text{Zn}(\text{BTZ})_2]_2$ at 329 nm; this feature may be related to the ability of the latter compound to exist as a dimer in the solid. Extinction coefficients for the longest wavelength absorption bands in the partially fluorinated systems (**19** and **20**) were larger than either $[\text{Zn}(\text{BTZ})_2]_2$ or fully fluorinated **21**; this is

consistent with an enhanced transition dipole moment consequent on selective fluorination.

b. Photoluminescence Studies. Photoluminescence spectra were recorded on powders, thus avoiding the complications due to solvation in the solution phase measurements and interference effects in thin film studies. The zinc enolates **5** and **6** both show broad visible luminescence upon excitation at 405 nm, with a central peak at around 500 nm and additional peaks at higher and lower wavelengths (Figure 7). Comparison

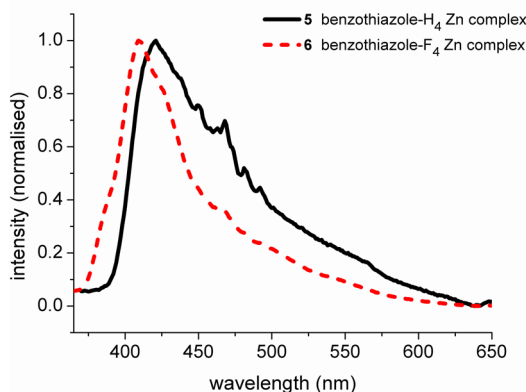
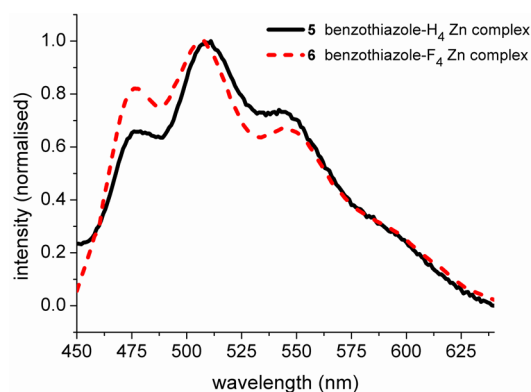


Figure 7. Photoluminescence emission spectra of powdered zinc enolates **5** and **6** upon excitation at 405 nm (top) and at 342 nm (bottom).

of the two photoluminescence emission spectra indicates that tetrafluorination of the ligands has only a slight effect on the peak wavelengths but does change their relative intensities. A similar emission spectrum has been observed by Fernández et al. for a gold(I) 2-(diphenylphosphino)-4,5,6,7-tetrafluorobenzothiazole complex,²⁰ and the structure of the band has been attributed to the involvement of a vibrational mode of the benzothiazole ring. Excitation of **5** and **6** at 342 nm, close to their UV absorption maxima, gives broad emissions, peaking at shorter wavelengths than when the excitation is at 405 nm (Figure 7). This dependence of the emission spectrum upon the excitation wavelength may arise because the observed spectra contain contributions from both fluorescence and phosphorescence; time-resolved studies of the luminescence are currently under way. The copper(II) enolate complex **7** does not show visible photoluminescence.

The photoluminescence spectrum of each of the phenoxides $[\text{Zn}(\text{BTZ})_2]_2$, **19**, **20** and **21**, excited at 368 nm, comprises a single broad peak in the visible region (Figures 8 and 9). Compared to emission from the nonfluorinated complex

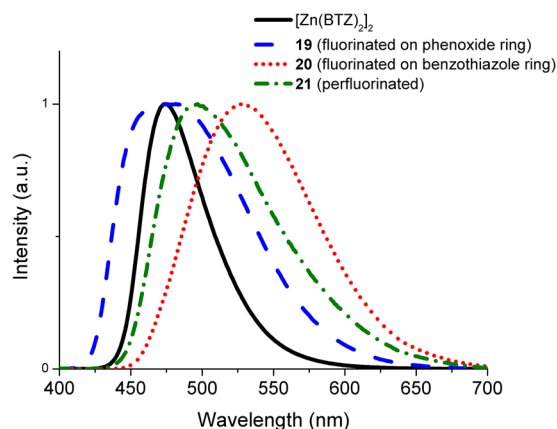


Figure 8. Photoluminescence emission spectra of powdered zinc phenoxides $[\text{Zn}(\text{BTZ})_2]_2$, **19**, **20**, and **21** upon excitation at 368 nm.

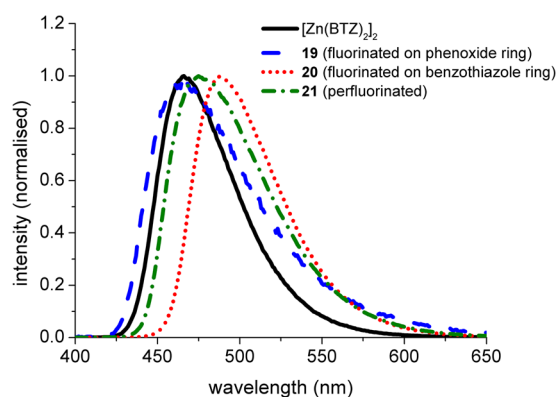


Figure 9. Photoluminescence emission spectra of zinc phenoxides $[\text{Zn}(\text{BTZ})_2]_2$, **19**, **20**, and **21** in DMSO solution upon excitation at 368 nm.

$[\text{Zn}(\text{BTZ})_2]_2$ at 474 nm, tetrafluorination on the phenoxide ring, to give **19**, hardly changes the peak wavelength but gives a broadened emission with the maximum at 476 nm. Tetrafluorination on the benzothiazolyl ring to give **20** leads to a red shift to 529 nm, whereas octafluorinated **21** shows an emission at 497 nm lying between the two tetrafluorinated complexes.

It is notable that the powder phase photoluminescence emission peaks of compounds **19–21** are broader than that of $[\text{Zn}(\text{BTZ})_2]_2$; the differences in peak widths are much less marked in DMSO solution, suggesting that this phenomenon is related to the structures adopted in the solid state. The compounds in which the phenoxide and benzothiazole rings are closest to coplanarity in the crystal, and so might be expected to have the most extensively delocalized π systems, are also the ones with the broadest emission peaks (Table 3). This relationship also applies in a comparison of enolates **5** and **6**, where the less highly fluorinated material gives the broader emission upon excitation at 342 nm.

Luminescence quantum yields for solutions of the zinc complexes in DMF were determined as detailed in the Supporting Information. The values calculated for complexes **20** and **21** approach that of the highly luminescent material $[\text{Zn}(\text{BTZ})_2]_2$, whereas compounds **5**, **6**, and **19** gave much lower quantum yields.

Table 3. Inverse Correlation between Dihedral Angles and Photoluminescence Full Width at Half Maximum (FWHM)

complex	5	6	$[\text{Zn}(\text{BTZ})_2]_2$	19	20	21
largest benzothiazole-(ph)enolate dihedral angle /deg	3.8	6.2	12.7	1.6	3.4	8.7
fwhm/nm	74	51	54	103	101	93

COMPUTATIONAL STUDIES

We have performed DFT calculations on the zinc complexes (Table 4). The HOMO and LUMO of the enolates **5** and **6** are delocalized but reside mainly on the ligands (Figure 10). Tetrafluorination of the benzothiazole rings lowers the energies of both these molecular orbitals by approximately 0.4 eV and leaves the HOMO–LUMO gap essentially unchanged. This is consistent with the experimental observations that compounds **5** and **6** have very similar absorption and photoluminescence spectra.

The electronic structures of monomeric and dimeric forms of nonfluorinated $\text{Zn}(\text{BTZ})_2$ were the subject of previous calculations.^{2,19} The HOMOs are mainly localized on the phenoxide rings, whereas the LUMOs are less localized and spread over both the benzothiazole and phenoxide rings. In the case of the dimer, the energy gap between the HOMO and LUMO is smaller than for the monomer; however, the HOMOs are located on the two bridging ligands, whereas the LUMOs are associated with the nonbridging ligands, so there may only be a low probability of a transition occurring between these particular orbitals. In Table 4, we present the results of our own DFT calculations for the monomer of $\text{Zn}(\text{BTZ})_2$ and the series of fluorinated analogues. The forms of the HOMO and LUMO wave functions are exemplified in Figure 11 by the perfluorinated zinc enolate **21**. Fluorination of just the phenoxide ring, to give **19**, reduces both the HOMO and LUMO energies by nearly equal amounts, relative to the hypothetical nonfluorinated monomer. On the other hand, fluorination of only the benzothiazole ring stabilizes the LUMO (delocalized over both rings) more than the HOMO (localized on the phenoxide ring), so that **20** has a decreased HOMO–LUMO gap compared with **19**, as is consistent with the red shift in both the absorption and photoluminescence spectra of **20**. Complete fluorination in **21** is calculated to provide a HOMO–LUMO gap almost equal to that in **20**; however the absorption spectrum of **21** is blue-shifted relative to **20** and more closely resembles that of **19**. Photoluminescence from **21** is also blue-shifted relative to **20**.

CONCLUSIONS

We have established efficient synthetic routes to fluorinated analogues of the 2-(2-hydroxyphenyl) ligand and have used Zn(II) to exemplify the formation of thermally stable, sublimable, photoluminescent metal complexes from these new ligands. The compounds have mononuclear, centrosymmetric structures in which stacking of π systems is observed. Partially fluorinated systems can give rise to $\pi_{\text{H}}-\pi_{\text{F}}$ stacking, but $\pi_{\text{H}}-\pi_{\text{H}}$ and $\pi_{\text{F}}-\pi_{\text{F}}$ assemblies are also observed. Fluorination of the aromatic rings in these ligands substantially lowers the HOMO and LUMO energies, whereas the changes in the wavelengths of visible absorption and of photoluminescence are comparatively subtle. These are attractive materials for the construction of OLEDs, since considerable variation of the electrical properties is possible.

The electroluminescence of the zinc complexes, their incorporation into OLEDs, and the coordination chemistry of the ligands with other metals, particularly the IR-emissive lanthanide ions such as Er^{3+} , are currently under investigation in our laboratories.

Table 4. Calculated HOMO and LUMO Energies for Zinc Enolate and Phenoxide Complexes

	5	6	Zn(BTZ) ₂	19	20	21
$E_{\text{LUMO}}/\text{eV}$	−1.94	−2.36	−1.79	−2.26	−2.19	−2.65
$E_{\text{HOMO}}/\text{eV}$	−6.01	−6.39	−5.39	−5.83	−5.68	−6.14
$\Delta E_{\text{LUMO-HOMO}}/\text{eV}$	4.07	4.03	3.61	3.58	3.49	3.48

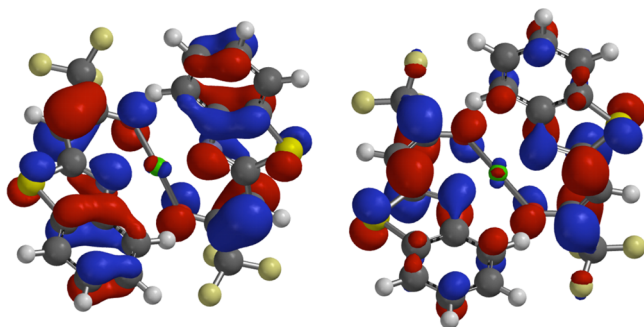


Figure 10. HOMO (left) and LUMO (right) of the zinc enolate 5.

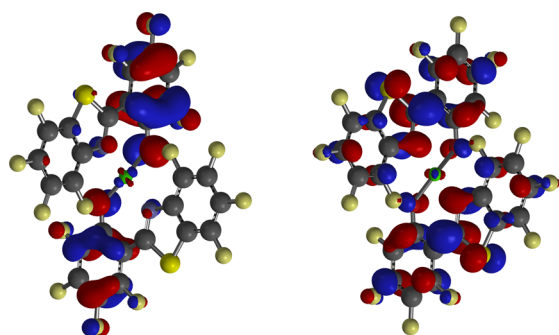


Figure 11. HOMO (left) and LUMO (right) of the fully fluorinated zinc phenoxide 21.

EXPERIMENTAL SECTION

General Procedures. Flash chromatography was performed using Zeochem ZEOprep 60 silica gel (40–63 μm). IR spectra were obtained by attenuated total reflectance (ATR) on a Perkin-Elmer Spectrum 65 FT-IR spectrometer. Mass spectra were recorded by the EPSRC National Service Mass Spectrometry Service Centre at Swansea. DFT calculations were performed using the Spartan'10 software package, version 1.0.1, using the DFT RB3LYP method with the 6-31G(D) basis set.

4,5,6,7-Tetrafluoro-2-(3,3,3-trifluoro-2-oxopropyl)benzothiazole (4b). 4,5,6,7-Tetrafluoro-2-methylbenzothiazole¹² (0.378 g, 1.7 mmol) in THF (10 mL) was treated with NaH (60% dispersion in oil; 68 mg, 1.7 mmol) at 0 °C with stirring. After 10 min, ethyl trifluoroacetate (0.45 mL, 3.77 mmol) was added, and the mixture was allowed to attain room temperature over 3 h. Hydrochloric acid (2 M; 2 mL), brine (5 mL), and Et₂O were added. The organic extracts were dried (Na₂SO₄), concentrated, and recrystallized (CHCl₃) to give the title compound 4b (0.20 g, 36%) as a white solid, mp 194–195 °C. Found: C, 37.32; H, 0.75; N, 4.30. C₁₀H₂F₇NOS·0.25H₂O requires C, 37.34; H, 0.78; N, 4.35%. UV (MeCN): λ_{max} 202 (ϵ 23500), 255 (9300), 307 (9200), 363 (22000); $\nu_{\text{max}}/\text{cm}^{-1}$ (ATR) 2606 (br), 1737, 1443, 1363, 1238, 1188, 1136, 1087, 1005, 883, 793, 730; δ_{H} (270 MHz, CDCl₃) 6.3 (1H, s, CH), 8.7 (1H, br, OH); δ_{F} (376 MHz, CDCl₃) −74.6 (s, CF₃), −139.0 (dd, J 20, 14 Hz), −148.6 (dd, J 19, 14 Hz), −156.6 (t, J 19.5 Hz), −158.2 (t, J 20 Hz). HRMS (EI) m/z found: 316.9745. C₁₀H₂F₇NOS (M⁺) requires 316.9740.

Zinc Complex of 2-(3,3,3-Trifluoro-2-oxopropyl)benzothiazole (5). A solution of 2-(3,3,3-trifluoro-2-oxopropyl)benzothiazole¹¹ 3b (0.50 g, 2.04 mmol) in boiling MeOH (20 mL) was mixed with a solution of Zn(OAc)₂·2H₂O (0.20 g, 0.91 mmol) in MeOH (5 mL).

The white precipitate was filtered off and recrystallized from chloroform to give 5 (0.41 g, 72%) as a white solid, mp 283–285 °C. Found: C, 43.35; H, 1.78; N, 5.13. C₂₀H₁₀F₆N₂O₂S₂Zn requires C, 43.38; H, 1.82; N, 5.06%. UV (MeCN): λ_{max} 211 (ϵ 46700), 268 (20900), 342 (53900); $\nu_{\text{max}}/\text{cm}^{-1}$ (ATR) 1624, 1573, 1492, 1458, 1418, 1281, 1185, 1109, 889, 749, 696; δ_{H} (400 MHz, CDCl₃) 6.25 (2H, s), 7.28 (2H, 'd', J 8.3 Hz), 7.31 (2H, td, J 7.6, 1.5 Hz), 7.36 (2H, td, J 7.6, 1.4 Hz), 7.75 (2H, 'd', J 7.7 Hz); δ_{F} (376 MHz, CDCl₃) −75.6. HRMS (EI) m/z found: 551.9379. C₂₀H₁₀F₆N₂O₂S₂Zn (M⁺) requires 551.9380.

Zinc Complex of 4,5,6,7-Tetrafluoro-2-(3,3,3-trifluoro-2-oxopropyl)benzothiazole (6). A solution of 4,5,6,7-tetrafluoro-2-(3,3,3-trifluoro-2-oxopropyl)benzothiazole (4b) (0.60 g, 1.89 mmol) in MeOH (15 mL) was mixed with a solution of Zn(OAc)₂·2H₂O (0.20 g, 0.91 mmol) in MeOH (5 mL). The white precipitate was filtered off and recrystallized from EtOAc–Et₂O (4:1) to give 6 (0.35 g, 53%) as a white solid, mp 290 °C. Found: C, 34.31; H, 0.10; N, 3.49. C₂₀H₂F₁₄N₂O₂S₂Zn requires C, 34.43; H, 0.29; N, 4.01%. UV (MeCN): λ_{max} 206 (ϵ 48500), 267 (14200), 347 (54500); $\nu_{\text{max}}/\text{cm}^{-1}$ (ATR) 1563, 1493, 1414, 1291, 1188, 1150, 1120, 1093, 1013, 920, 881, 777, 695; δ_{H} (270 MHz, CDCl₃) 6.4 (s, CH); δ_{F} (376 MHz, CDCl₃) −75.8 (s, CF₃), −139.0 (dd, J 20.4, 14.3 Hz), −153.4 (dd, J 20.2, 14.1 Hz), −155.5 (t, J 19.5 Hz), −158.7 (t, J 20.3 Hz). HRMS (EI) m/z found: 695.8627. C₂₀H₂F₁₄N₂O₂S₂Zn (M⁺) requires 695.8623.

Copper Complex of 4,5,6,7-Tetrafluoro-2-(3,3,3-trifluoro-2-oxopropyl)benzothiazole (7). A solution of 4,5,6,7-tetrafluoro-2-(3,3,3-trifluoro-2-oxopropyl)benzothiazole (4b) (0.061 g, 0.19 mmol) in MeOH (5 mL) was mixed with a solution of Cu(OAc)₂·H₂O (0.028 g, 0.14 mmol) in MeOH (5 mL). The precipitate was filtered off and recrystallized from EtOH–Et₂O to give 7 (0.050 g, 74%) as deep violet crystals, mp 285 °C. UV–vis (MeCN): λ_{max} 209 (ϵ 57100), 256 (16200), 351 (41600), 426 (52), 515 (41), 730 (86); $\nu_{\text{max}}/\text{cm}^{-1}$ (ATR) 1560, 1491, 1396, 1286, 1198, 1123, 1090, 1016, 926, 880, 797, 696. HRMS (EI) m/z found: 694.8629. C₂₀H₂CuF₁₄N₂O₂S₂ (M⁺) requires 694.8625.

N-(Pentafluorophenyl)-2-methoxybenzamide (8). A solution of 2-methoxybenzoyl chloride (0.85 g, 0.74 mL, 5.0 mmol) in DCM (12 mL) was added dropwise to a solution of pentafluoroaniline (1.83 g, 10.0 mmol) in DCM (12 mL). The mixture was stirred at room temperature for 24 h, after which an additional portion of pentafluoroaniline (0.1 mmol) was added to ensure complete consumption of the acyl chloride. After a further 5 h, the solvent was evaporated, and the resulting residue was recrystallized from chloroform to give N-pentafluorophenyl-2-methoxybenzamide 8 (1.53 g, 96%) as a white solid, mp 161.5–163 °C. $\nu_{\text{max}}/\text{cm}^{-1}$ (ATR) 3301 (N–H), 1673 (C=O), 1655, 1602, 1519, 1458, 1290, 1231, 1186, 1096, 1048, 981, 759; δ_{H} (270 MHz, CDCl₃) 7.07 (1H, d, J 8 Hz), 7.14 (1H, t, J 8 Hz), 7.55 (1H, t, J 8 Hz), 8.26 (1H, d, J 8 Hz), 9.38 (1H, s, NH); δ_{F} (376 MHz, CDCl₃) −145.5 (2F, m), −158.8 (1F, t, J 20 Hz), −163.9 (2F, m). HRMS (ESI) m/z found: 318.0551. C₁₄H₉F₅NO₂ (M+H⁺) requires 318.0548.

N-(Pentafluorophenyl)-3,4,5,6-tetrafluoro-2-methoxybenzamide (9). 2-Methoxy-3,4,5,6-tetrafluorobenzoyl chloride²² (2.79 g, 11.5 mmol) in DCM (70 mL) was added dropwise to a solution of pentafluoroaniline (4.39 g, 24 mmol) in DCM (35 mL) over 20 min under N₂. The mixture was stirred at room temperature under N₂ for 24 h; then the solvent was evaporated at reduced pressure. The resulting residue was recrystallized from CHCl₃–petrol to give amide 9 (3.48 g, 78%) as a white, fluffy solid, mp 114–115.5 °C. $\nu_{\text{max}}/\text{cm}^{-1}$ 3225, 1686, 1488, 1320, 1239, 1150, 991, 641; δ_{H} (400 MHz, CDCl₃) 4.08 (3H, s, OMe), 7.78 (1H, br s, NH); δ_{F} (376 MHz, CDCl₃) −139.2 (1F, d, J 22 Hz), −144.2 (2F, d, J 22 Hz), −149.8 (1F, t, J 22

Hz), -154.7 (1F, qt, J 22, 11 Hz), -155.2 (2F, t, J 22 Hz), -160.4 (1F, t, J 22 Hz), -161.8 (1F, t, J 22 Hz). HRMS (CI) m/z found: 390.0171. $C_{14}H_3F_8NOS$ ($M+H^+$) requires 390.0169.

4,5,6,7-Tetrafluoro-2-(2-methoxyphenyl)benzothiazole (10). P_2S_5 (0.27 g, 1.2 mmol) and N -(pentafluorophenyl)-2-methoxybenzamide (8) (1.2 g, 3.8 mmol) were refluxed under N_2 in dry dioxane (10 mL) for 24 h. The solvent was evaporated, and the residue was dissolved in chloroform and washed with aqueous $NaHCO_3$. The organic extract was dried ($MgSO_4$) and evaporated, leaving **10** (1.191 g, 100%) as a pale orange solid, mp $204-206$ °C. ν_{max}/cm^{-1} (ATR) 2843, 1598, 1583, 1484, 1454, 1440, 1351, 1287, 1256, 1231, 1163; δ_H (270 MHz, $CDCl_3$) 4.11 (3H, s, OMe), 6.98–7.15 (2H, m), 7.36–7.50 (1H, m), 8.42 (1H, dd, J 7.9, 1.5 Hz); δ_F (377 MHz, $CDCl_3$) -140.7 (1F, dd, J 20.5, 15.4 Hz), -150.1 (1F, dd, J 19.0, 15.6 Hz), -160.2 (1F, t, J 19.3 Hz), -161.0 (1F, t, J 20.1 Hz). HRMS (ESI) m/z found: 314.0260. $C_{14}H_8F_4NOS$ ($M+H^+$) requires 314.0257.

2-(3,4,5,6-Tetrafluoro-2-methoxyphenyl)-4,5,6,7-tetrafluorobenzothiazole (11). N -(Pentafluorophenyl)-3,4,5,6-tetrafluoro-2-methoxybenzamide (9) (3.03 g, 7.79 mmol) and P_2S_5 (865 mg, 3.89 mmol) were refluxed in dry dioxane (80 mL) under N_2 for 20 h. The solvent was evaporated, and the residue was extracted with ether and washed with aqueous $NaHCO_3$. The organic phase was dried over Na_2SO_4 , filtered, and evaporated. The resulting pale yellow solid was subjected to flash chromatography (gradient from petroleum-DCM 6:1 to 4:1) to give **11** (2.14 g, 71%) as a white solid, mp $110-111$ °C. ν_{max}/cm^{-1} 1637, 1490, 1467, 1346, 1088, 998, 885, 820, 747; δ_H (270 MHz, $CDCl_3$) 4.08 (s, OMe); δ_F (367 MHz, $CDCl_3$) -137.6 (1F, ddd, J 22, 9, 5 Hz), -139.3 (1F, dd, J 21, 16 Hz), -147.6 (1F, dd, J 19, 16 Hz), -150.8 (1F, td, J 21, 5 Hz), -156.3 (1F, dd, J 21, 9 Hz), -158.1 (1F, t, J 19 Hz), -158.4 (1F, t, J 19 Hz), -162.5 (1F, t, J 21 Hz). HRMS (EI) m/z found: 384.9801. $C_{14}H_3F_9NO_2$ (M^+) requires 384.9802.

4,5,6,7-Tetrafluoro-2-(2-hydroxyphenyl)benzothiazole (12). BBr_3 (3.0 mL, 32 mmol) was added to a solution of 4,5,6,7-tetrafluoro-2-(2-methoxyphenyl)benzothiazole (10) (1.00 g, 3.19 mmol) in DCM (16 mL). The mixture was stirred under N_2 at room temperature for 3 h and then poured onto ice. The resulting suspension was extracted with chloroform, which was dried (Na_2SO_4), then concentrated under a vacuum to give **12** as a white solid (960 mg, 100%), mp $181-183$ °C. Found: C, 52.26; H, 1.48; N, 4.51. $C_{13}H_5F_4NOS$ requires C, 52.18; H, 1.68; N, 4.68.

UV (MeCN): λ_{max} 288 (ϵ 18400), 335 (16800); ν_{max}/cm^{-1} (ATR) 2950 (O–H), 1550, 1490, 1230, 1020; δ_H (270 MHz, $CDCl_3$) 7.00 (1H, td, J 8.1, 1.4 Hz), 7.13 (1H, dd, J 8.1, 1.0 Hz), 7.46 (1H, td, J 8.1, 1.4 Hz), 7.64 (1H, dd, J 8.1, 1.4 Hz), 11.62 (1H, s, OH); δ_F (376 MHz, $CDCl_3$) -139.2 (1F, dd, J 23, 15 Hz), -148.6 (1F, dd, J 21, 15 Hz), -157.8 (1F, t, J 21 Hz), -158.9 (1F, t, J 21 Hz). HRMS (APCI) m/z found: 300.0101. $C_{13}H_6F_4NOS$ ($M+H^+$) requires 300.0101.

2-(3,4,5,6-Tetrafluoro-2-hydroxyphenyl)-4,5,6,7-tetrafluorobenzothiazole (13). BBr_3 (4 mL, 42 mmol) was added to a solution of 2-(3,4,5,6-tetrafluoro-2-methoxyphenyl)-4,5,6,7-tetrafluorobenzothiazole (1.00 g, 2.60 mmol) in DCM (16 mL). The mixture was stirred at room temperature for 2 h and then poured onto ice (150 g). The resulting suspension was extracted with DCM twice and ether once. The combined organic phases were dried over Na_2SO_4 and evaporated to leave **13** as a yellowish-white solid (960 mg, 99%), mp $158-159$ °C. ν_{max}/cm^{-1} 1668, 1542, 1489, 1437, 1406, 1353, 1270, 1144, 1100, 1050, 988, 750; δ_H (270 MHz, $CDCl_3$) 8.01 (br, OH); δ_F (367 MHz, $CDCl_3$) -138.8 (1F, dd, J 20, 15 Hz), -139.4 (1F, dt, J 22, 8 Hz), -147.8 (1F, t, J 17 Hz), -149.2 (1F, td, J 15, 6 Hz), -156.0 (1F, t, J 20 Hz), -156.3 (1F, t, J 20 Hz), -161.4 (1F, ddd, J 20, 9, 4 Hz), -170.3 (1F, td, J 19, 4 Hz). HRMS (EI) m/z found: 370.9650. $C_{14}H_5F_8NOS$ (M^+) requires 370.9646.

2-(3,4,5,6-Tetrafluoro-2-hydroxyphenyl)benzothiazole (16). **Method A.** A mixture of 2-aminothiophenol (14) (1.35 g, 10.8 mmol) and 3-ethoxycarbonyl-2-methyl-5,6,7,8-tetrafluoro-4H-1,4-dihydrobenzopyran-4-one²³ (15) (0.820 g, 2.70 mmol) in dry toluene (32 mL) was refluxed under N_2 overnight. After cooling, the yellow precipitate was filtered off and recrystallized from toluene to yield a bright yellow solid (0.115 g), which was indicated to be a mixture by 1H NMR. Flash chromatography (petrol-DCM, 4:1) gave **16** as a pale

yellow solid (48 mg, 6%), mp $226-228$ °C (lit.¹³ $193-195$ °C). ν_{max}/cm^{-1} (ATR) 1644 (br), 1500, 1418, 986, 761. UV (MeCN): λ_{max} 292 (ϵ 18500), 325 (16700); δ_H (400 MHz, $DMSO-d_6$) 7.60 (1H, t, J 7.5 Hz), 7.67 (1H, t, J 7.5 Hz), 8.24 (1H, d, J 7.5 Hz), 8.29 (1H, d, J 7.5 Hz), 13.51 (1H, s, OH); δ_F (376 MHz, $DMSO-d_6$) -139.9 (1F, d, J 22 Hz), -152.9 (1F, m), -162.3 (1F, m), -171.1 (1F, m). HRMS (APCI) m/z found: 300.0095. $C_{13}H_6F_4NOS$ ($M+H^+$) requires 300.0101.

The above procedure was repeated, starting with 2-aminothiophenol (14) (1.00 g, 8.02 mmol) and pyrone derivative **15** (1.22 g, 4.01 mmol), but instead of using flash chromatography, purification of the crude product was attempted by repeated recrystallization from toluene. 2-(2-Benzothiazol-2-yl-1-hydroxyvinyl)-3,4,5,6-tetrafluorophenol (17) (54 mg, 4%) was obtained as a bright yellow solid, mp >200 °C (decomp). ν_{max}/cm^{-1} (ATR) 3157, 1658, 1521, 1432, 1204, 1146, 987, 926, 749, 720, 686; δ_H (400 MHz, $DMSO-d_6$) 6.75 (1H, s), 7.34 (1H, t, J 8 Hz), 7.44–7.60 (2H, m), 7.96 (1H, d, J 8 Hz), 13.59 (1H, br, OH), 15.63 (1H, br, OH); δ_F (376 MHz, $DMSO-d_6$) -139.7 (1F, m), -154.0 (1F, m), -165.2 (1F, m), -173.2 (1F, m). HRMS (APCI) m/z found: 342.0203; $C_{15}H_8F_4NO_2S$ ($M+H^+$) requires 342.0206.

Method B. 2-Methoxy-3,4,5,6-tetrafluorobenzoyl chloride (0.50 g, 2.0 mmol) was added dropwise to a solution of 2-aminothiophenol (14) (0.26 g, 2.0 mmol) in N -methyl-2-pyrrolidone (2 mL). The mixture was stirred at 100 °C under N_2 for 24 h and then poured into water. The precipitate was filtered off and washed with water. After drying, it was recrystallized from chloroform and further purified by dry flash chromatography ($CHCl_3$ –hexane 2:3, preheated before use). The early product-containing fractions were combined and evaporated to give **16** as a flaky, lemon-yellow solid (253 mg, 42%), with mp, IR, 1H NMR, and ^{19}F NMR data in agreement with those for **16** prepared by method A above. Found: C, 52.09; H, 1.68; N, 4.56. $C_{13}H_5F_4NOS$ requires: C, 52.18; H, 1.68; N, 4.68%.

Zinc Complex of 2-(2-Hydroxy-3,4,5,6-tetrafluorophenyl)benzothiazole (19). To a boiling solution of 2-(3,4,5,6-tetrafluoro-2-hydroxyphenyl)benzothiazole (16) (23.8 mg, 0.0796 mmol) in MeOH (50 mL) was added 0.1 M methanolic KOH (0.79 mL, 0.0796 mmol), followed by a solution of $Zn(OAc)_2 \cdot 2H_2O$ (8.72 mg, 0.0398 mmol) in MeOH (5 mL). A yellow precipitate gradually formed, and the mixture was kept boiling and stirring for another 45 min, after which the precipitate was filtered off and washed with boiling MeOH to yield **19** as a bright yellow, fluffy solid (21.1 mg, 80%), mp >400 °C. Found: C, 47.25; H, 1.25; N, 4.18. $C_{26}H_8F_8N_2O_2S_2Zn$ requires: C, 47.18; H, 1.22; N, 4.23%. ν_{max}/cm^{-1} (ATR) 1656, 1481, 1404, 1259, 998, 750; λ_{max} (DMSO) 398 (40200), 281 (24000); δ_H (400 MHz, $DMSO-d_6$) 8.34 (1H, d, J 8 Hz), 8.06 (1H, d, J 8 Hz), 7.40–7.49 (2H, m); δ_F (376 MHz, $DMSO-d_6$) -141.7 (m), -141.8 (m), -157.6 (m), -163.7 (m). HRMS (APCI) m/z found: 660.9269. $C_{26}H_9F_8N_2O_2S_2Zn$ ($M+H^+$) requires 660.9264.

Zinc Complex of 4,5,6,7-Tetrafluoro-2-(2-hydroxyphenyl)benzothiazole (20). To a solution of 4,5,6,7-tetrafluoro-2-(2-hydroxyphenyl)benzothiazole (12) (0.30 g, 1 mmol) in chloroform (15 mL) was added 1 M KOH in MeOH (1 mL, 1 mmol). The resultant bright yellow precipitate was filtered off and washed with chloroform to give the potassium salt of ligand **12** (0.286 g, 85%). A portion of this potassium salt (68 mg, 0.2 mmol) was dissolved in MeOH (3 mL) and mixed with a solution of $Zn(OAc)_2 \cdot 2H_2O$ (11 mg, 0.1 mmol) in MeOH (0.5 mL). The mixture was refluxed for 12 min, and the resultant yellow precipitate was filtered off, washed with MeOH, and dried. The filtrate was concentrated under a vacuum to give a second crop of precipitate, which was combined with the first crop to give the zinc complex **20** (50.7 mg, 77%), mp >400 °C. Found: C, 47.29; H, 1.61; N, 4.02. $C_{26}H_8F_8N_2O_2S_2Zn$ requires: C, 47.18; H, 1.22; N, 4.23%. ν_{max}/cm^{-1} (ATR) 1480, 1417, 1198, 1013, 883; λ_{max} (DMSO) 431 (ϵ 42500), 295 (23500); δ_H (400 MHz, $DMSO-d_6$) 8.22 (1H, d, J 8 Hz), 7.23 (1H, t, J 8 Hz), 7.09 (1H, d, J 8 Hz), 6.67 (1H, t, J 8 Hz); δ_F (376 MHz, $DMSO-d_6$) -140.5 (m), -151.3 (m), -161.0 (m), -163.2 (m). HRMS (APCI) m/z found: 660.9265. $C_{26}H_9F_8N_2O_2S_2Zn$ ($M+H^+$) requires 660.9264.

Zinc Complex of 2-(3,4,5,6-Tetrafluoro-2-hydroxyphenyl)-4,5,6,7-tetrafluorobenzothiazole (21). To a boiling solution of ligand **13** (649 mg, 1.75 mmol) in 1:1 Et₂O–MeOH was added 1 M KOH in MeOH (1.80 mL, 1.80 mmol); the color changed from pale yellow to bright yellow at once. After 5 min, the solvent was evaporated, and the bright yellow residue was dissolved in boiling water. To the resultant solution was added aqueous Zn(OAc)₂·2H₂O (287 mg, 1.31 mmol). A bright yellow precipitate formed immediately. After 30 min, the mixture was filtered while hot; the precipitate was washed with boiling water and dried to give zinc complex **21** (645 mg, 92%), mp 338–340 °C. Found: C, 38.61; H, <0.10; N, 3.64. C₂₆F₁₆N₂O₂S₂Zn requires C, 38.76; H, 0.00; N, 3.47%. λ_{max} (DMSO) 404 (ϵ 31900), 282 (23100); δ_{F} (376 MHz, CD₃OD) –141.4 (m), –142.7 (m), –149.3 (m), –157.7 (m), –161.8 (m), –162.5 (m), –166.3 (m), –181.6 (m). HRMS (APCI) m/z found 826.8329. C₂₆F₁₆N₂NaO₂S₂Zn (M+Na⁺) requires 826.8329.

■ ASSOCIATED CONTENT

■ Supporting Information

Molecular structures of enolate complexes **5** and **7**, molecular structures of phenoxide complexes **19** and **20**, emission of perfluorinated zinc phenolate **21** in different solvents, measurements of fluorescence quantum yield. This material is available free of charge via the Internet at <http://pubs.acs.org>.

■ AUTHOR INFORMATION

Corresponding Author

*E-mail: p.b.wyatt@qmul.ac.uk.

Notes

The authors declare no competing financial interest.

■ ACKNOWLEDGMENTS

We thank Mr. G. Coumbarides for NMR spectroscopy, the EPSRC National Mass Spectrometry Service Centre, Swansea for MS measurements, the EPSRC National Crystallography Service, Southampton for data collection, the EPSRC and the Royal Academy of Engineering (vacation bursary for J.M., fellowship for I.H.), and the China Scholarships Council (studentships for Z.L., Y.P., and H.Y.).

■ REFERENCES

- (1) Ugarova, N. N.; Brovko, L. Y. *Luminescence* **2002**, *17*, 321–330.
- (2) Yu, G.; Yin, S.; Liu, Y.; Shuai, Z.; Zhu, D. *J. Am. Chem. Soc.* **2003**, *125*, 14816–14824.
- (3) Wu, X.-M.; Hua, Y.-L.; Wang, Z.-Q.; Zheng, J.-J.; Feng, X.-L.; Sun, Y.-Y. *Chin. Phys. Lett.* **2005**, *22*, 1797–1799.
- (4) Xu, X.; Liao, Y.; Yu, G.; You, H.; Di, C.; Su, Z.; Ma, D.; Wang, Q.; Li, S.; Wang, S.; Ye, J.; Liu, Y. *Chem. Mater.* **2007**, *19*, 1740–1748.
- (5) Bingshe, X.; Huixia, X.; Liuqing, C.; Xiaohong, F.; Xuanguang, L.; Hua, W. *Org. Electron.* **2008**, *9*, 267–272.
- (6) Roh, S.-G.; Kim, Y.-H.; Seo, K. D.; Lee, D. H.; Kim, H. K.; Park, Y. I.; Park, J. W.; Lee, J. H. *Adv. Funct. Mater.* **2009**, *19*, 1663–1671.
- (7) Sakamoto, Y.; Suzuki, T.; Kobayashi, M.; Gao, Y.; Fukai, Y.; Inoue, Y.; Sato, F.; Tokito, S. *J. Am. Chem. Soc.* **2004**, *126*, 8138–8140.
- (8) Zhou, J.; Liang, Q.; Dong, J. *Carbon* **2010**, *48*, 1405–1409.
- (9) (a) Chen, B.; Chen, B.; Yang, Y.; Zapata, F.; Qian, G.; Luo, Y.; Zhang, J.; Lobkovsky, E. B. *Inorg. Chem.* **2006**, *45*, 8882–8886. (b) Winkless, L.; Tan, R. H. C.; Zheng, Y.; Motevalli, M.; Wyatt, P. B.; Gillin, W. P. *Appl. Phys. Lett.* **2006**, *89*, 111115.
- (10) Berger, R.; Resnati, G.; Metrangolo, P.; Weber, E.; Hulliger, J. *Chem. Soc. Rev.* **2011**, *40*, 3496–3508.
- (11) Kawase, M.; Teshima, M.; Saito, S.; Tani, S. *Heterocycles* **1998**, *48*, 2103–2110.
- (12) Herkes, F. E. *J. Fluorine Chem.* **1979**, *13*, 1–21.
- (13) Bazyl', I. T.; Kasil', S. P.; Burgart, Y. V.; Saloutin, V. I. *J. Fluorine Chem.* **2000**, *103*, 3–12.
- (14) Brembilla, A.; Roizard, D.; Lochon, P. *Synth. Commun.* **1990**, *20*, 3379–3384.
- (15) Melman, J. H.; Rohde, C.; Emge, T. J.; Brennan, J. G. *Inorg. Chem.* **2002**, *41*, 28–33.
- (16) Buzzeo, M. C.; Iqbal, A. H.; Long, C. M.; Millar, D.; Patel, S.; Pellow, M. A.; Saddoughi, S. A.; Smenton, A. L.; Turner, J. F. C.; Wadhawan, J. D.; Compton, R. G.; Golen, J. A.; Rheingold, A. L.; Doerrer, L. H. *Inorg. Chem.* **2004**, *43*, 7709–7725.
- (17) Collings, J. C.; Smith, P. S.; Yufit, D. S.; Batsanov, A. S.; Howard, J. A. K.; Marder, T. B. *CrystEngComm* **2004**, *6*, 25–28.
- (18) Cozzi, F.; Bacchi, S.; Filippini, G.; Pilati, T.; Gavezzotti, A. *Chem.—Eur. J.* **2007**, *13*, 7177–7184.
- (19) Collings, J. C.; Roscoe, K. P.; Thomas, R. L.; Batsanov, A. S.; Stimson, L. M.; Howard, J. A. K.; Marder, T. B. *New J. Chem.* **2001**, *25*, 1410–1417.
- (20) Fernández, E. J.; Laguna, A.; López-de-Luzuriaga, J. M.; Monge, M.; Montiel, M.; Olmos, M. E.; Rodríguez-Castillo, M. *Dalton Trans.* **2006**, 3672–3677.
- (21) Qureshi, M.; Manoharan, S. S.; Singh, S. P.; Mahapatra, Y. N. *Solid State Commun.* **2005**, *133*, 305–309.
- (22) Kasil', S. P.; Burgart, Y. V.; Saloutin, V. I.; Chupakhin, O. N. *J. Fluorine Chem.* **2001**, *108*, 125–131.
- (23) Kasil', S. P.; Burgart, Y. V.; Saloutin, V. I. *Russ. J. Org. Chem.* **2001**, *37*, 1455–1462.